FEBS 24483 FEBS Letters 489 (2001) 171–175

Structure/function of human herpesvirus-8 MIP-II (1–71) and the antagonist N-terminal segment (1–10)[1]

Matthew P. Crump[a,2], Elena Elisseeva[a], Jiang-Hong Gong[b], Ian Clark-Lewis[b], Brian D. Sykes[a,*]

[a] *Protein Engineering Network of Centers of Excellence (PENCE) and Department of Biochemistry, 713 Heritage Medical Research Center, University of Alberta, Edmonton, Alta., Canada T6G 2S2*
[b] *Biomedical Research Centre and Department of Biochemistry and Molecular Biology, University of British Columbia, Vancouver, B.C., Canada V6T 1Z3*

Received 3 November 2000; revised 27 November 2000; accepted 27 November 2000

First published online 21 December 2000

Edited by Thomas L. James

Abstract Kaposi's sarcoma-associated herpesvirus encodes a chemokine called vMIP-II that has been shown to be a broad range human chemokine receptor antagonist. Two N-terminal peptides, vMIP-II(1–10) and vMIP-II(1–11)dimer (dimerised through Cys11) were synthesised. Both peptides are shown to bind the CXC chemokine receptor 4 (CXCR4). vMIP-II(1–10) was 1400-fold less potent than the native protein whilst the vMIP-II(1–11)dimer was only 180-fold less potent. In addition, both peptides are CXCR4 antagonists. Through analysis of non-standard, long mixing time two-dimensional nuclear Overhauser enhancement spectroscopy experiments, ^{13}C relaxation data and amide chemical shift temperature gradients for the N-terminus of vMIP-II, we show that this region populates a turn-like structure over residues 5–8, both in the presence and absence of the full protein scaffold. This major conformation is likely to be in fast exchange with other conformational states but it has not previously been detected in monomeric chemokine structures. This and other studies [Elisseeva et al. (2000) J. Biol. Chem. 275, 26799–26805] suggest that there may be a link between the structuring of the short N-terminal chemokine peptides and their ability to bind their receptor.

Key words: Chemokine; vMIP-II; CXC chemokine receptor 4; Peptide analog; Nuclear magnetic resonance

1. Introduction

Immune cell trafficking comprises circulation, homing and adhesion, extravasation and recirculation of discrete populations of leukocytes between the blood vessels, lymph and lymphoid organs [1]. An entire superfamily of chemoattractant cytokine (chemokines) proteins and their receptors are involved in the molecular regulation of trafficking [2]. Chemokine activities on leukocyte sub-populations are mediated through the binding and activation of seven transmembrane helix G-coupled receptors and nine distinct functional human CC chemokine receptors (CCR(1–9)) and five CXC chemokine receptors (CXCR(1–5) have been identified [3]. The chemokines therefore play a pivotal role in the control of leukocyte chemotaxis and represent attractive targets for the blockade of inflammatory disease progression [4]. They are however also targets for viral agents that attempt to subvert the normal host immune response. Kaposi's sarcoma (KS) is a tumour-like lesion that has become frequent in immunodeficient individuals [5]. KS-associated herpesvirus is the infectious agent responsible for KS and interestingly it has been found to encode several proteins that have direct human immune system counterparts [6]. In particular, two open reading frames code for CC chemokine-like proteins that have approximately 40% identity to the human CC chemokines. One of these, vMIP-II, has been shown to bind and block receptors belonging to the CXC, CC and XC class, blocking the normal calcium response elicited through receptors CCR1, CCR2, CCR5, CCR8, CXCR4 and XCR1 [7,8]. vMIP-II is a potent agonist of CCR3 [9] and also stimulates weak activity through the CXCR2 (IL-8B) receptor [7].

The structural basis for promiscuous receptor recognition is not well understood. The chemokine structures solved to date are remarkably homogeneous, containing a central core of three β-strands and an overlying C-terminal α-helix [2]. In the monomeric subunits, the strands are preceded by a disordered N-terminus, the CXC or CC disulphide motif and an extended loop (termed N-loop). Many structure/function stud-

*Corresponding author. Fax: (1)-780-492 1473. E-mail: brian.sykes@ualberta.ca

[1] The atomic coordinates for the family of 55 peptide structures for vMIP-II(1–10) have been deposited in the Protein Data Bank, Brookhaven National Laboratory, Upton, NY, USA with access code 1hff. The atomic coordinates of the minimised average structure and restraint files of full length vMIP-II (1–71) have been deposited in the Protein Data Bank, Brookhaven National Laboratory, Upton, NY, USA with access code 1hfg and r1hfgmr and the family of 38 structures with code 1hfn. Chemical shifts have been deposited in the BioMagResBank with access code 4914.
[2] Present address: Department of Biochemistry, University of Southampton, Bassett Crescent East, Southampton SO16 7PX, UK

Abbreviations: CCR, CC chemokine receptor; CXCR, CXC chemokine receptor; NMR, nuclear magnetic resonance; DQF-COSY, double-quantum-filtered correlated spectroscopy; TOCSY, total correlation spectroscopy; NOESY, two-dimensional nuclear Overhauser enhancement spectroscopy; NOE, nuclear Overhauser enhancement; vMIP-II(1–10), the peptide consisting of the N-terminal residues ^{1}LGASWHRPDK^{10}; vMIP-II(1–11)dimer, the peptide consisting of the N-terminal residues ^{1}LGASWHRPDKC^{11}, dimerised through Cys11

0014-5793/01/$20.00
PII: S0014-5793(00)02393-0

ies aimed at characterising regions of the chemokine fold that are important for function have concluded that the N-terminus, the disulphide motif and the N-loop are essential for binding and triggering of the receptor [10]. Modifications and deletions within these regions have generated analogues that still bind but do not signal and so act as receptor antagonists [11]. It is within these regions that vMIP-II shows the greatest divergence from its closest human CC chemokine relative MIP-1α and it may be the case that these regions control the promiscuous receptor binding.

The N-terminus, the disulphide motif and the N-loop are essential for binding and triggering of the receptor and are the least well defined regions of the chemokine structure. Therefore in this study we have focused on the N-terminus of vMIP-II (vMIP-II(1–10)) both in the absence and presence of the remaining protein scaffold. These studies reveal that the N-terminus alone is sufficient for CXCR4 receptor binding and furthermore it is a receptor antagonist. The formation of a dimer of residues (1–9) of SDF-1 was recently shown to increase CXCR4 binding when compared to monomeric (1–9) [12] and we go on to show that the binding is increased by the formation of a dimer consisting of the first 11 residues of the N-terminus of vMIP-II, disulphide linked through Cys11. However in this case the binding is two-fold stronger than the SDF-1(1–9)dimer binding. This has prompted a detailed nuclear magnetic resonance (NMR) study of vMIP-II(1–10) using two-dimensional (2D) methods, long mixing time 2D nuclear Overhauser enhancement spectroscopy (NOESY) experiments, the temperature gradients of amide proton chemical shifts and ^{13}C relaxation data. We show that although the vMIP-II(1–10) peptide is flexible, the NMR data reveals a major family of structures consisting of a turn, both in the free peptide and the full vMIP-II structure (also presented herein). This feature is not observed during the application of standard NMR methods to solving the full protein structure. The turn is stabilised principally by the packing of the Trp5 (tryptophan is not observed in any other chemokine N-terminus) against the side chains of both Arg7 and Pro8.

2. Materials and methods

2.1. Chemical synthesis of vMIP-II and peptides (1–10) and (1–11)dimer

Peptides were synthesised as described previously [13]. The (1–11) peptide was dimerised via a disulfide bridge formed by gentle oxidation of the cysteines using 10% Me_2SO in water.

2.2. Cell culture

The CEM cell line was purchased from the American Type Culture Collection (Rockville, MD, USA) and maintained in RPMI 1640 medium supplemented with 10% foetal calf serum.

2.3. Chemotaxis

Migration of CEM cells was performed with disposable Transwell trays (Costar, Cambridge, MA, USA, with 6.5 mm diameter chambers and a membrane pore size of 3 μm). The agonist/antagonist, in HEPES-buffered RPMI 1640 supplemented with 10 mg/ml^{-1} bovine serum albumin (0.6 ml) was added to the lower well, and 0.1 ml of CEM cells (1×10^7 ml^{-1}) in the same medium without agonist was added to the upper wells. After 2 h, cells that migrated to the lower wells were counted. Chemotactic migration was determined by the subtraction of cells migrated in medium alone. All assays were performed in duplicate.

2.4. vMIP-II receptor binding

Competition for binding of ^{125}I-labelled SDF-1 to CEM cells was carried out as described in [11].

2.5. NMR studies of vMIP-II(1–10)

^1H NMR spectra of the vMIP-II(1–10) were acquired at 600 MHz using a Varian Unity spectrometer. Double-quantum-filtered correlated spectroscopy (DQF-COSY), total correlation spectroscopy (TOCSY) and NOESY spectra were used to fully assign the ^1H resonances. All spectra were acquired at 8°C in 90% H_2O/10% D_2O or 99.99% D_2O. For the determination of the solution conformation of vMIP-II(1–10), NOESY spectra at mixing times of 125, 300, 400 and 500 ms were used and build-up rates were found to be linear over this range. $\{^1H\}$-^{13}C nuclear Overhauser enhancement (NOE) experiments that focused on Cα protons were performed at 600 MHz on a sample of vMIP-II(1–10) at 281 and 308 K.

2.6. Structure determination of vMIP-II(1–10)

NOE peaks picked from the 8°C, 500 ms NOESY data set were integrated and converted to distance restraints. The restraints were grouped as strong, medium, weak and very weak classes corresponding to upper distance restraints of 2.8, 3.5, 4.5 and 5.5 Å, respectively. Upper distance restraints were corrected with centre averaging where appropriate for non-stereospecifically assigned methylene protons. A total of 105 NOEs were assigned corresponding to 40 sequential, 13 short range and 52 intra residue restraints. Structure calculations were performed using the simulated annealing protocols within XPLOR [14] and utilised 4000 steps of high temperature dynamics (1000 K) and 4000 cooling steps to a final temperature of 298 K. The NOE force constant was set at 50 kcal mol^{-1} Å^2. Out of 100 calculated structures, 55 were selected that showed no NOE violations >0.2 Å.

2.7. NMR studies of vMIP-II (1–71)

NMR experiments were performed on Varian Unity 600 and Varian Inova 500 and 600 MHz spectrometers at temperatures ranging from 8 to 35°C. Samples for structural studies were 2 mM protein, 20 mM sodium acetate, 1 mM sodium azide and 1 mM DSS at pH 5.0. Standard pulse sequences were employed for resonance assignments: DQF-COSY, TOCSY and NOESY. TOCSY spectra were acquired with mixing times of 55 ms and NOESY spectra with mixing times of 50, 150, 300 and 500 ms (300 and 500 ms datasets were used for the analysis of residues 1–10 only).

2.8. Structure calculations for vMIP-II(1–74)

The solution structure of vMIP-II was determined as described previously [11] using the dynamic simulated annealing protocol within the program X-PLOR [14]. A total of 777 NOEs were used in the structure calculations comprised of 201 long range ($|i-j|\geq5$), 57 short range ($4\geq|i-j|\geq1$), 191 sequential ($|i-j|=1$) and 306 intra residues ($i=j$). A set of 38 final structures was selected from the 40 refined structures on the basis of lowest total energy and agreement with the experimental data. Analysis of the (ϕ, ψ) backbone torsion angles and quality of the structures was made using the program PROCHECK [15].

3. Results and discussion

3.1. Receptor binding of the vMIP-II N-terminal peptides

Previously several peptides SDF(1–9) and SDF(1–9)dimer [12] and several vMIP-II N-terminal peptides (including (1–10), (6–18) and (1–21)) have been shown to have weak binding to CXCR4 [16]. In this study residues 1–10 of the N-terminus of vMIP-II (-LGASWHRPDK-), vMIP-II(1–10) and (1–11) (-LGASWHRPDKC-) and the vMIP-II(1–11)dimer were synthesised and tested for chemotaxis and receptor binding. CEM cells were used to determine the binding of the vMIP-II N-terminal peptides to CXCR4. The competition for binding of ^{125}I-labelled native SDF-1 by unlabelled SDF-1, SDF(1–9), SDF(1–9)dimer, vMIP-II(1–10) and vMIP-II(1–11)dimer is shown in Fig. 1A. SDF(1–9) shows the weakest binding and competition by the SDF-1(1–9) is incomplete at the concen-

trations tested. An accurate K_d could not be calculated but was estimated as 1500-fold less than wild-type binding [12]. However, the vMIP-II(1–10) shows stronger binding than the SDF(1–9) monomeric counterpart and binds 1400 times less tightly than SDF-1. The most dramatic increases in binding come from the dimeric forms, the SDF(1–9)dimer and vMIP-II(1–11)dimer. In the study by Loetscher et al. [12], the SDF(1–9)dimer showed only 82-fold less binding than native SDF-1. In the present assays the binding is shown to be 300-fold weaker than SDF-1 and slightly lower than seen before. However, the binding of vMIP-II(1–11)dimer is only 180-fold less than SDF-1 and is the most tightly binding small peptide that we have observed to date. As controls, the N-terminal

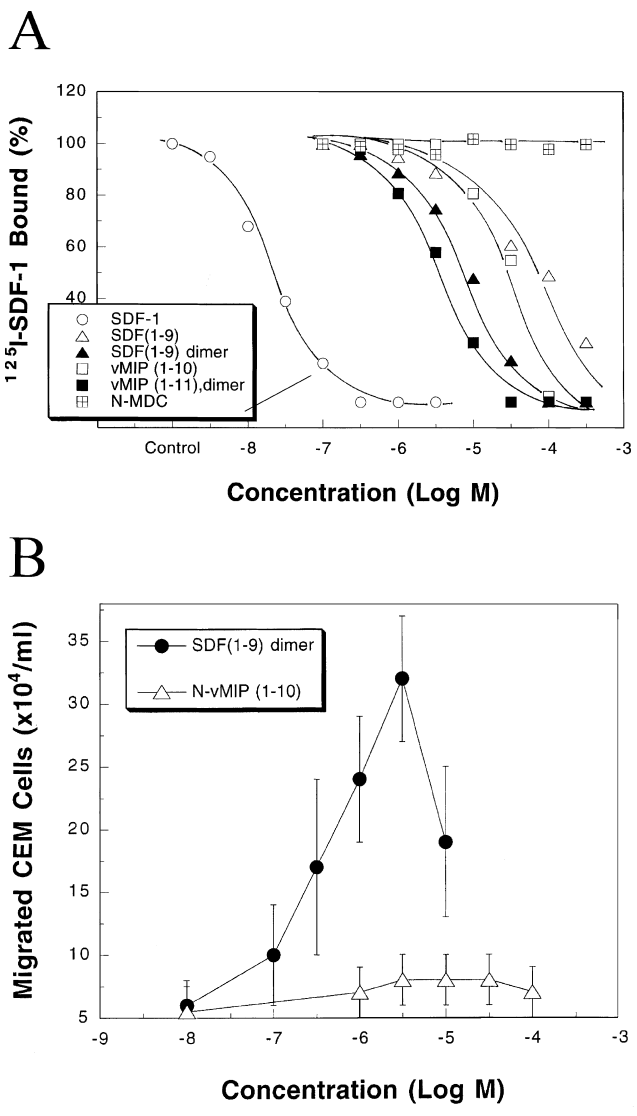

Fig. 1. Receptor binding of vMIP-II and SDF-1 based N-terminal peptides and chemotaxis inhibition by vMIP-II(1–10). A: Competition for specific binding of ^{125}I-SDF-1 (4 nM) to CEM cells by SDF-1 (open circle), SDF(1–9) monomer (open triangle), SDF-(1–9)dimer (closed triangle), vMIP-II(1–10) (open square), vMIP-II(1–11)dimer (closed square) and N-MDC (square with cross). The data for the N-terminal peptides of IP-10, eotaxin and eotaxin-2 are not shown. The results are representative of duplicate experiments. B: CEM cell migration induced by concentrations of SDF-(1–9)dimer (closed circle) and the antagonist vMIP-II(1–10) (open triangle). Data are the means of ±S.D. of duplicate determinations from two separate experiments.

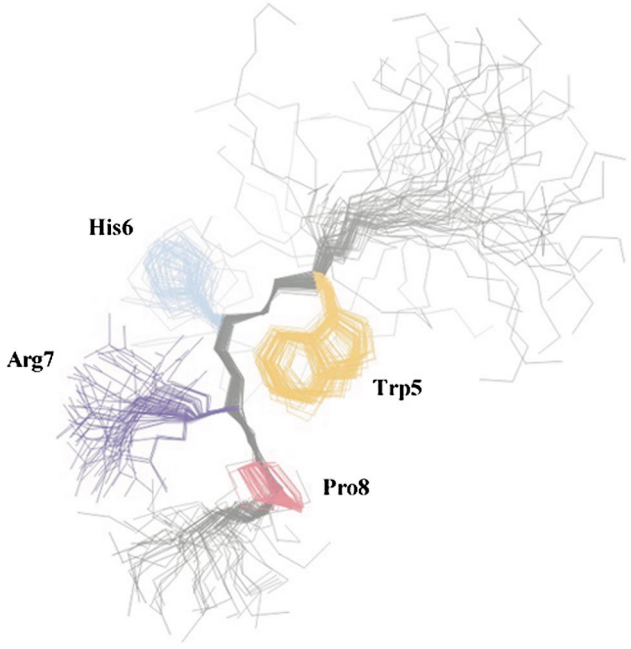

Fig. 2. Solution structure of the vMIP-II(1–10). A bundle of 55 calculated structures is shown superimposed on the average structure. Residues Trp5 through to Pro8 corresponding to the region of partial structuring are annotated.

peptides from MDC, IP-10, eotaxin and eotaxin-2 were synthesised and also tested for competitive binding of ^{125}SDF-1 to CXCR4. Data for MDC is shown in Fig. 1A. This is representative of each peptide tested and shows that no receptor binding is observed. This indicates that binding of short peptides to CXCR4 is not a general property of either CXCR4 or this type of short peptide ligand.

3.2. vMIP-II(1–10) does not induce chemotaxis

Since native vMIP-II is an antagonist for CXCR4, we next tested whether the antagonistic properties were retained by the N-terminal fragments. Fig. 1B shows chemotaxis inhibition data for vMIP-II(1–10) and SDF-(1–9)dimer. vMIP-II(1–10) did not induce chemotaxis of CEM cells whereas SDF-(1–9)dimer induced a dose-dependent chemotaxis. Therefore, despite receptor binding, the N-terminal peptide does not appear to activate the CXCR4 receptor and importantly, retains its antagonist properties.

3.3. 3D structure of vMIP-II (1–10)

^{1}H NMR assignments for the vMIP-II(1–10) were made using standard 2D NMR techniques. Subsequently, a total of 105 NOEs could be assigned from an 8°C NOESY corresponding to 40 sequential, 13 short range and 52 intra residue restraints. The principal contacts that define the 3D structure are the 13 short range NOEs between the Trp5 ring and the side chain of Arg7/Pro8, between Arg7 and Asp9, Val3 and Trp5 and Ser4 and His6. A total of 100 structures were calculated of which 55 were selected that contained no NOE restraint violations >0.2 Å. Examination of the 55 structures showed that they are clustered with almost identical backbone conformation over residues 5–8 (Fig. 2). The formation of a small hydrophobic pocket appears to centre around a tryptophan staple between Trp5 and Pro8. For these residues, sev-

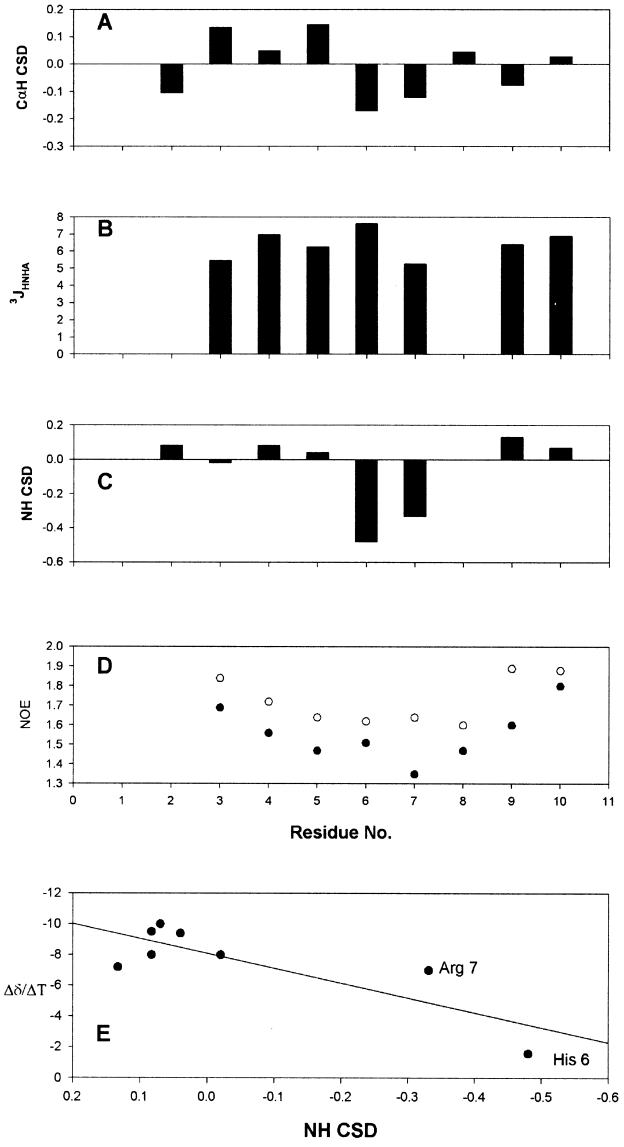

Fig. 3. NMR structural characterisation of vMIP-II(1–10). A: CαH CSD from random coil values. B: Measured three bond HN–HA ($^3J_{HNHA}$) coupling constant. C: NH CSD from random coil values. D: ^{1}H-{^{13}C} NOE at 30 and 8°C. E: Plot of amide temperature coefficients versus amide CSD. The line shows the best fit to the data with linear regression with slope −9.6 ppt/°C and a correlation coefficient of 0.67.

eral short range (*i*, *i*+3) NOEs were detected between the side chain ring protons of Trp5 and the proline ring. In addition (*i*, *i*+2) NOEs between backbone and side chain protons of Arg7 to the ring of Trp5 define the earlier portion of the chain. It should be stressed however that our use of restraints in these calculations is only giving us information on the folded form and this is likely to be in equilibrium with numerous unfolded states that we are not detecting with NOESY experiments (i.e. $\langle R^{-6}\rangle$ averaging of the NOE may bias the short distance contacts that most likely arise in a folded form). Analysis of the backbone CαH and NH (Fig. 3A,B) chemical shifts shows that little or no deviation is seen for the CαH chemical shifts but both His6 and Arg7 show deviation in the more sensitive NH chemical shifts. Backbone $^3J_{HNHA}$ coupling constants are mostly averaged through the peptide (6–8 Hz) with the exception of Arg7 that shows a reduced coupling constant (5.3 Hz). Natural ^{13}C abundance {^{1}H}-^{13}C NOE experiments for vMIP-II(1–10) were also recorded and the data analysed specifically for the relaxation of the backbone Cα protons. Fig. 3D compares values measured at 30 and 8°C. A smaller NOE (η) value indicates reduced motion and a larger η indicates greater motion on a picosecond timescale. At 30°C residues Ala3, Ser4, Asp9 and Lys10 and the ends of the peptide show increased values of η whilst the central four residues show reduced values. This suggests that the ends of the peptide are somewhat more flexible than the central positions as expected. When the temperature is reduced to 8°C all of the NOE values drop, due in part to an increase in the viscosity of the water. However some increases are particularly prominent, i.e. for Arg7 and Asp9. The overall dip in the NOE values at the centre of the peptide versus the ends also increases significantly compared to the 30°C data, indicating an increase in overall structuring of the central portion of the peptide.

A recent study by Andersen et al., [17] shows extensively that the $\Delta\delta/\Delta T$ versus chemical shift deviation (CSD) of the amide proton correlated well with partial structuring of the peptides which then become increasingly randomised upon warming. In general fits with slopes between −8 and 20 ppt/°C and high correlation coefficients ($R^2 > 0.7$) were observed for short peptides with well characterised structuring at lower temperatures. To measure the $\Delta\delta/\Delta T$ values for vMIP-II-(1–10), a series of 1D spectra were measured at a range of temperatures between 8 and 30°C. The CSDs for vMIP-II-(1–10) were derived from the lowest temperature set included (8°C) and were corrected according to Anderson [17] and Wishart [18]. Fig. 3E shows the resulting plot of CSD versus $\Delta\delta/\Delta T$ for vMIP-II(1–10). The majority of residues show little CSD and large $\Delta\delta/\Delta T$ gradients and lie in a cluster with the clear exception again of His6 and Arg7. When fit with linear regression, we obtained a slope of −9.6 ppt/°C and a correlation coefficient *R* of 0.67 giving the expected correlation for a minimally structured protein fragment.

3.4. 3D structure of the N-terminus within vMIP-II(1–71)

We have solved the full 3D structure of vMIP-II(1–71) at 30°C and deposited the coordinates, restraints and structural statistics in the Brookhaven PDB with access number 4914. At 30°C and at 150 ms mixing times, we observed no short range NOEs within the N-terminus with the exception of two extremely weak NOEs between the Trp5 ring and the δHs of Pro8. However NOESY experiments at 30 and 8°C with 500 ms mixing times showed a set of short range NOEs within the N-terminus similar to those observed in the (1–10) peptide. In several cases spectral overlap and poorer spectral quality prevented an NOE comparison being made in the 8°C dataset of vMIP-II(1–71). Nevertheless these experiments confirm that the structuring we observed in the free peptide may also be detected with long mixing time experiments in the context of the full protein structure. The remaining 3D structure of vMIP-II was broadly confirmatory of other chemokine structures and in the absence of thorough structure/function data we have not given a comparison of vMIP-II with other chemokines that share the similar receptors (eotaxin CCR3, SDF-1 CXCR5). A detailed comparison has been presented elsewhere in the literature [19].

Little or no binding has been observed between the N-ter-

minal fragments of chemokines and the chemokine receptors suggesting that numerous interactions are required to ensure strong binding. The exceptions to this rule are the N-terminal domains of vMIP-II and SDF-1 that showed binding to CXCR4, albeit weakly. Both peptides bound to CXCR4 more strongly when they were disulphide linked to form a dimer. For SDF-1(1–9) this improved the binding from 1500-fold less than native SDF-1, to only 82-fold less for SDF-1(1–9)dimer. The vMIP-II(1–11)dimer shows the strongest binding yet observed for an N-terminal fragment. This may be a purely statistical factor (i.e. there is essentially double the concentration of N-terminal peptide) or, as we have described previously, one half of the dimer may mimic the N-loop of the full protein and interact with a second part of the receptor [20]. As seen in Fig. 1A, our success in steadily increasing the binding of short peptide sequences to CXCR4 warrants further investigation into the factors dictating the binding of this region.

In this report we have also shown by a combination of NMR structure determination methods that the vMIP-II-(1–10) samples a turn-like structure through residues 5 to 8. The extension of this approach to the use of long mixing time NOESY experiments with the full length protein has also allowed the identification of the same NOE patterns within the N-terminus of native vMIP-II(1–71). Structuring within an N-terminal peptide from the SDF-1 sequence has also recently been reported [20] over residues 5–8. Both of these studies have employed long mixing time NOESY experiments aimed at allowing sufficient NOE build-up in the partially structured regions that have effective short correlation times and slow NOE build-up rates. It is now an open question as to whether binding may be attributable to an increased propensity for a constitutive structure in this region. This is part of ongoing studies in our laboratory which continue to address the role of the N-terminus in receptor binding.

Acknowledgements: We thank Philip Owen, Luen Vo, Michael Williams and Paul Semchuk for chemical synthesis. We acknowledge Gerry McQuaid for maintenance of the spectrometers. We thank Lewis Kay for pulse sequences.

References

[1] Springer, T.A. (1994) Cell 76, 301–314.
[2] Baggiolini, M., Dewald, B. and Moser, B. (1997) Ann. Rev. Immunol. 15, 675–705.
[3] Luster, A.D. (1998) N. Engl. J. Med. 338, 436–445.
[4] Zack Howard, O.M., Ben-Baruch, A. and Oppenheim, J.J. (1996) Trends Biotechnol. 14, 46–51.
[5] Chang, Y., Cesarman, E., Pessin, M.S., Lee, F., Culpepper, J., Knowles, D.M. and Moore, P.S. (1994) Science 266, 1865–1869.
[6] Moore, P.S., Boshoff, C., Weiss, R.A. and Chang, Y. (1996) Science 274, 1739–1744.
[7] Kledal, T.N., Rosenkilde, M.N., Coulin, F., Simmons, G., Johnsen, A.H., Alouani, S., Power, C.A., Luttichau, H.R., Gerstoft, J., Clapham, P.R., Clark-Lewis, I., Wells, T.N.C. and Schwartz, T.W. (1997) Science 277, 1656–1659.
[8] Shan, L., Qiao, X., Oldham, E., Catron, D., Kaminski, H., Lundell, D., Zlotnik, A., Gustafson, E. and Hedrick, J.A. (2000) Biochem. Biophys. Res. Commun. 268, 938–941.
[9] Boshoff, C., Endo, Y., Collins, P.D., Takeuchi, Y., Reeves, J.D., Schwieckart, V.L., Siani, M.A., Sasaki, T., Williams, T.J., Gray, P.W., Moore, P.S., Chang, Y. and Weiss, R.A. (1997) Science 278, 290–294.
[10] Clark-Lewis, I., Kim, K.-S., Rajarathnam, K., Gong, J.-H., Dewald, B., Moser, B., Baggiolini, M. and Sykes, B.D. (1995) J. Leuk. Biol. 57, 703–711.
[11] Crump, M.P., Gong, J.-H., Loetscher, P., Rajarathnam, K., Amara, A., Arenzana-Seisdedos, F., Virelizier, J.-L., Baggiolini, M., Sykes, B.D. and Clark-Lewis, I. (1997) EMBO J. 16, 6996–7007.
[12] Loetscher, P., Gong, J.-H., Dewald, B., Baggiolini, M. and Clark-Lewis, I. (1998) J. Biol. Chem. 35, 22279–22283.
[13] Clark-Lewis, I., Vo, L., Owen, P. and Anderson, J. (1997) Methods Enzymol. 287, 233–250.
[14] Brünger, A.T. (1993) X-PLOR Manual (Version 3.1), Yale University, New Haven, CT.
[15] Lakowski, R.A., MacArthur, M.W. and Thornton, J.M. (1993) J. Appl. Crystallogr. 26, 283–291.
[16] Zhou, N., Luo, Z., Luo, J., Hall, J.W. and Huang, Z. (2000) Biochemistry 39, 3782–3787.
[17] Andersen, N.H., Neidigh, J.W., Harris, S.M., Lee, G.M., Liu, Z. and Tong, H. (1997) J. Am. Chem. Soc. 119, 8547–8561.
[18] Wishart, D.S., Bigam, C.G., Holm, A., Hodges, R.S. and Sykes, B.D. (1995) J. Biomol. NMR 5, 67–81.
[19] LiWang, A.C., Wang, Z.-X., Sun, Y., Peiper, S.C. and Liwang, P.J. (1999) Prot. Sci. 8, 2270–2280.
[20] Elisseeva, E.L., Slupsky, C.M., Crump, M.P., Clark-Lewis, I. and Sykes, B.D. (2000) J. Biol. Chem. 275, 26799–26805.